STRONGLY-PERTURBED NON-EQUILIBRIUM GAS PHYSICS MODEL FOR THE PARAXIAL DIODE TRANSPORT CELL*

S. Strasburg[ℵ], D.D. Hinshelwood, D. Mosher,
J.W. Schumer, and P. F. Ottinger
Plasma Physics Division, Naval Research Laboratory, Washington, DC 20375

Abstract

Intense short-pulse charged-particle beams—those with tens or hundreds of kA/cm^2 and beam risetimes less than 100 ns— can disturb the background gas so severely that not only are diatomic molecules ionized, but molecules may be dissociated and the product atoms themselves multiply ionized. Such beam-background systems are generally far from temperature and species equilibrium. The plasma conductivity σ, which is determined by the degree of ionization and the species temperatures, strongly influences the beam behavior through the plasma return current. Thus, simultaneously and self-consistently solving for both σ and the beam propagation is essential for a correct description of the system behavior. A plasma physics model with advanced gas chemistry has been developed and incorporated into the simulation code LSP to help meet this objective.

I. INTRODUCTION

The intense electron beam generated by a paraxial diode[1,2] can deposit of order 1 J/cm^3 in the downstream 1-10 Torr air transport cell in less than 50 ns. Such large energy densities and short time scales require a theoretical and computational physics model which can accurately handle molecular dissocation, multiply ionized atoms, and non-equilibrium populations. Correctly modeling the conductivity of the background plasma is critical for determining beam stopping and the plasma return current $\boldsymbol{J_p}$. The magnitude and radial dependence of $\boldsymbol{J_p}$ in turn affect the bremsstrahlung spot size, beam transverse temperature, optimal location of the target, and, finally, the radiation output.

The gas-physics method described here extends an earlier LSP[3] scalar conductivity swarm model which was compared to experiment through theory and computation[4]. In the present model, rate equations for three molecular species and all atomic charge states are solved simultaneously with two energy balance equations to determine the temperatures of electrons and heavy particles. It is found that for low energy-density deposition, the excitation of molecular degrees of freedom controls the level of dissociation and ionization of the primary diatomic components of air, N_2 and O_2. For higher energy-density deposition—corresponding to longer beams, rarer background gases, or higher beam current densities—the background gas is fully dissociated, has an average atomic charge state of unity or greater (background electron densities ~10^{17} cm^{-3}), and has a high plasma electron temperature (~5 eV). A time-dependent coronal model, balancing collisional ionization with radiative recombination, is appropriate for this parameter regime. The combination of dissociation physics and coronal modeling allows the extension of the conductivity model to severely-disturbed gases characteristic of paraxial diodes.

An NRL Gamble II paraxial diode experiment[1] has conducted laser interferometry, time-resolved spot size, target energy-deposition calorimetry, and net-current measurements of a 1.4 MV, 40 kA electron beam in the gas transport cell. Comparisons of these results both with theory and the extended gas-physics model incorporated in the computational code LSP are discussed. The computer code also presents future opportunities to study pre-ionization of the transport gas and advanced paraxial-diode geometries. Since interferometry techniques from NRL will soon be used to diagnose electron densities in paraxial diodes[2] for the first time, the physics understanding gained by the present campaign should prove valuable for optimizing the performance of a diode which has previously been empirically studied.

II. MODEL DETAILS

The gas-physics model described here consists of three primary components: (A) rate equations for approximately ten nitrogen species, (B) energy equations for electron and heavy species temperatures, and (C) the determination of plasma properties such as collision frequencies and conductivity. The predecessor to this model[4] assumed an undissociated gas with singly-ionized molecules, and used the *local-field approximation* for the electron temperature, so that $T_e = T_e(\varepsilon / p)$, where ε is the local electric field, and p is the background gas pressure. An initial attempt at a correction to this model included additional species without removing the local-

* Work supported by DOE through SNL, LANL, and LLNL.
ℵ NRC Postdoctoral Associate at NRL. Email: stras@suzie.nrl.navy.mil

Report Documentation Page

Form Approved
OMB No. 0704-0188

1. REPORT DATE	2. REPORT TYPE	3. DATES COVERED
JUN 2003	**N/A**	**-**

4. TITLE AND SUBTITLE	5a. CONTRACT NUMBER
Strongly-Perturbed Non-Equilibrium Gas Physics Model For The Paraxial Diode Transport Cell	5b. GRANT NUMBER
	5c. PROGRAM ELEMENT NUMBER
6. AUTHOR(S)	5d. PROJECT NUMBER
	5e. TASK NUMBER
	5f. WORK UNIT NUMBER
7. PERFORMING ORGANIZATION NAME(S) AND ADDRESS(ES) **Plasma Physics Division, Naval Research Laboratory, Washington, DC 20375**	8. PERFORMING ORGANIZATION REPORT NUMBER
9. SPONSORING/MONITORING AGENCY NAME(S) AND ADDRESS(ES)	10. SPONSOR/MONITOR'S ACRONYM(S)
	11. SPONSOR/MONITOR'S REPORT NUMBER(S)

12. DISTRIBUTION/AVAILABILITY STATEMENT
Approved for public release, distribution unlimited

13. SUPPLEMENTARY NOTES
See also ADM002371. 2013 IEEE Pulsed Power Conference, Digest of Technical Papers 1976-2013, and Abstracts of the 2013 IEEE International Conference on Plasma Science. IEEE International Pulsed Power Conference (19th). Held in San Francisco, CA on 16-21 June 2013. U.S. Government or Federal Purpose Rights License, The original document contains color images.

14. ABSTRACT
Intense short-pulse charged-particle beamsthose with tens or hundreds of kA/cm2 and beam risetimes less than 100 ns can disturb the background gas so severely that not only are diatomic molecules ionized, but molecules may be dissociated and the product atoms themselves multiply ionized. Such beam-background systems are generally far from temperature and species equilibrium. The plasma conductivity ó, which is determined by the degree of ionization and the species temperatures, strongly influences the beam behavior through the plasma return current. Thus, simultaneously and self-consistently solving for both ó and the beam propagation is essential for a correct description of the system behavior. A plasma physics model with advanced gas chemistry has been developed and incorporated into the simulation code LSP to help meet this objective.

15. SUBJECT TERMS

16. SECURITY CLASSIFICATION OF:			17. LIMITATION OF ABSTRACT	18. NUMBER OF PAGES	19a. NAME OF RESPONSIBLE PERSON
a. REPORT	b. ABSTRACT	c. THIS PAGE			
unclassified	**unclassified**	**unclassified**	**SAR**	**4**	

field assumption; when this was found to be inadequate, more detailed energy flow was considered.

(A) The model tracks the following nitrogen densities:

$$n_2^u,\ n_2^x,\ n_2^+,\ n^{(z)}.$$

These are, respectively, neutral molecules in the ground and excited state, singly-charged molecular ions, and z-times ionized atoms. Here, z ranges from 0 (a special case denoting neutral atoms) to Z, the atomic number. The average charge state of an *atom*, $\langle z \rangle$, is given by $\langle z \rangle\, n_a = \Sigma_z\, z\, n^{(z)}$, where $n_a = \Sigma_z\, n^{(z)}$ is the total number of atoms. Since *molecular* ions also contribute electrons, the total electron density is $n_e = \langle z \rangle\, n_a + n_2^+$. Rate equations for these species include excitation and de-excitation of neutral molecules; collisional dissociation of molecules, including contributions from all species; dissociative recombination ($N_2^+ + e \rightarrow N + N$); and thermal electron ionization of neutral molecules and atoms in all charge states. Many of these processes are augmented for excited neutral molecules due to their vibrational and electron-state potential energy. A density-dependent correction to the ionization of neutral atoms is included[5]. Other forms of recombination are too slow to be important on the beam time scale, but can easily be added. Beam processes (such as beam electron ionization) are included, but are generally small.

(B) The temperatures of the *electrons* and *heavy* species are followed through separate energy balance equations. The temperatures T and internal energies E are related by the equations $E_\alpha = 1.5\, n_\alpha\, T_\alpha$, where α denotes either e for electrons, or h for heavy particles, and n_h is the number density of nuclei, a constant. Energy flow from the beam to the background gas/plasma system is by direct beam deposition (proportional to beam current and roughly independent of beam energy between 100 kV and 5 MeV) and, generally much larger, ohmic heating (proportional to the plasma resistivity and the square of the plasma return current). Energy flow between the electron plasma and the heavy species is by collisional equilibration, by excitation of molecular degrees of freedom (including vibrational, rotational, and electron state), and by converting thermal-kinetic energy into potential energy of dissociation and ionization. The plasma is taken to be optically thin, so that radiation from deexcited atoms is lost from the system. At each time step, energy is deposited in the plasma, exchanged between species, and lost from the system, and then the two species temperatures are calculated from the two available kinetic energies. The electron and heavy species are assumed to be (separately) maxwellianized each time step.

(C) Plasma parameters are determined using the above quantities. Collision frequencies between all species are calculated from appropriate temperature- and density-dependent models, including separate Debye corrections for charged atoms and charged molecules. The plasma conductivity σ is proportional to n_e / ν (where ν is the total collision frequency), and is used in determining the plasma return current.

At each time step, then, charge-state averaged quantities such as $\langle z \rangle$ and n_e are calculated; temperatures T_e and T_h are derived from the energies E_e and E_h; frequencies of collision, equilibration, and species change are calculated; the plasma conductivity is calculated; power deposition and exchanges are determined and used to update the energies; and the rate equations for molecular and atomic species are applied. The variables n_2^u, n_2^x, n_2^+, $n^{(z)}$, E_e, and E_h, as well as σ, which is used in determining the return current, are then available for the following timestep.

This conductivity model yields substantial insight in a 0-D mode, but there are many features of physics experiments which are not captured by a model which neglects spatial dependence. These include the details of the beam radial profile; the location of the plasma return current; local contributions to this return current from $\sigma\, \vec{u} \times \vec{B}$ drifts, where u is the local mass plasma fluid velocity, and B is the local magnetic field; and the movement of the beam due to its own forces (mediated by the conducting background plasma), such as beam pinching and beam focus sweep. As an example, while the current density at a ring-diode cathode is below 20 kA/cm^2, under certain circumstances the beam is shown in the current simulations to pinch, leading to current densities of over 30 kA/cm^2. This drastically changes the local electron density, and, since the scaling of n_e with current density is nonlinear, can affect integrated line-of-sight measurements of n_e as well. The conductivity model was therefore incorporated into LSP, a multi-dimensional, fully electromagnetic, parallel, fluid/PIC code in order to more fully represent the beam-background physics.

II. PHYSICS REGIMES

As described above, in addition to the main source of energy— the ohmic heating P_Ω of the electrons—there are two primary energy sinks. These are excitation of molecular modes such as vibration and singlet/triplet states, $-P_m$, and energy lost to the ionization potential, $-P_z$. For undissociated gases, $-P_m$ is very large, balancing P_Ω so that energy deposited in the electrons is quickly equilibrated with internal molecular degrees of freedom. As the gas is dissociated, $-P_m$ becomes smaller in magnitude and the average charge state of atoms increases, so that P_Ω balances $-P_z$. The dividing line between dominance of the two energy sinks is determined by the *energy-density deposition*. Low energy-per-gas-particle systems are indicated by low beam current densities or high particle densities (*i.e.*, high pressures), and high energy systems by high current densities and low pressures.

Figure 1 shows the two regimes for a typical gas cell transporting a beam generated by a ring diode with current density 20 kA/cm^2 and beam pulse duration of 140 ns. (These plots display local quantities, which are different from the spatially-integrated measurements noted below.) In Fig. 1(a), a 10 Torr gas is shown by

simulation to be only partially dissociated by the peak of the beam current pulse, and electrons are contributed by both ionic molecules and singly-ionized atoms. In the 20 ns before and after the peak beam current at 70 ns, the electron temperature decreases from 3 to 2 eV. For the first 100 ns, P_Ω and $-P_m$ are closely balanced. Figure 1(b) shows, in contrast, a 1 Torr gas which has been dissociated within the first 30 ns of the pulse, and has completely burned through the z = 1 and 2 states and is starting in on the triply-ionized state, restricted only by the large ionization energy $-P_z$ required to reach this $\langle z \rangle$.

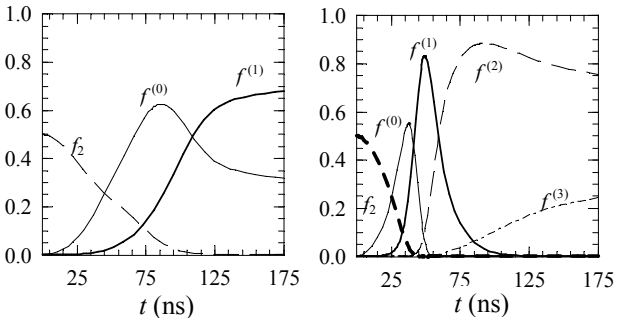

Fig. 1. Nitrogen-species fractions for 10 Torr (left) and 1 Torr ring-diode cells. Shown are neutral molecules and low atomic states.

The temperature range is considerably higher, 5 to 3 eV between 50 and 90 ns. (Another way for the plasma to distribute the energy absorbed ohmically by the electrons is through equipartition of the temperatures T_e and T_h. Equipartition is achieved for the cases in Fig. 1 near the end of the beam pulse.)

The atomic regime is further distinguished into singly-ionized and multiply-ionized (coronal) regimes. (The coronal regime is so called because of the importance of the coronal model assumptions[6] in deriving the ionization rates for the higher atomic states.) Figure 2 shows the plasma electron density at the end of the beam pulse as a function of beam current density, as predicted by the 0-D model. Background pressures from 0.5 to 40 Torr are shown. In the molecular and coronal regimes, n_e depends strongly on pressure, while for the singly-ionized regime the pressure dependence is weak or nonexistent. The molecular regime is characterized by a slight dissociation fraction, $f_d = n_a / 2n_2^0 < 0.5$, and a low electron density fraction, $f_e = n_e / 2n_2^0 < 0.25$. The atomic regime has $f_d \sim 1$ and $\langle z \rangle \sim 1$, while for the coronal regime $\langle z \rangle > 1.25$. The key independent variable distinguishing molecular, atomic, and coronal regimes is energy-density deposition, so that the parameter space of beam current density *vs*. background pressure is an appropriate domain for a plot of the dependent variables f_d and $\langle z \rangle$.

III. EXPERIMENTAL COMPARISON

Two recent experiments have measured ionization and net current fractions in gas cells transporting intense electron beams. A ring-diode experiment[4] used a two-color interferometer to analyze the effects of a 140 ns annular electron beam, extending from 6.5 to 7.5 cm radius, transporting 800 kA at 900 kV through 1 to 10 Torr air. In a second experiment, a paraxial diode generated a 30 kA, 1.4 MV electron beam whose effects in air, argon and helium were studied.[1]

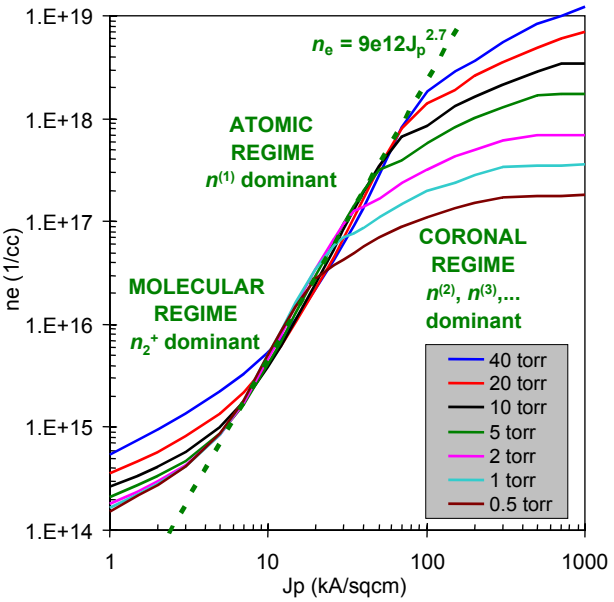

Fig. 2. Final n_e for various background pressures in a ring-diode cell, given by the 0-D model.

Previous studies of the ring-diode beam-induced ionization used a *scale factor* shifting the pressure to reproduce experimental results. The new model correctly reproduces experimental trends without this assumption, and is close to the quantitative experimental values. In Fig. 3, a plot of n_eL, the line density along the interferometric line-of-sight, is shown for the experiment, new model, and old model. The dramatically improved agreement argues that correctly following additional species and energy flow is critical to the plasma chemistry. The new model's slight underestimate of the electron density may be a consequence of the strong nonlinear dependence of the final value of n_e on beam

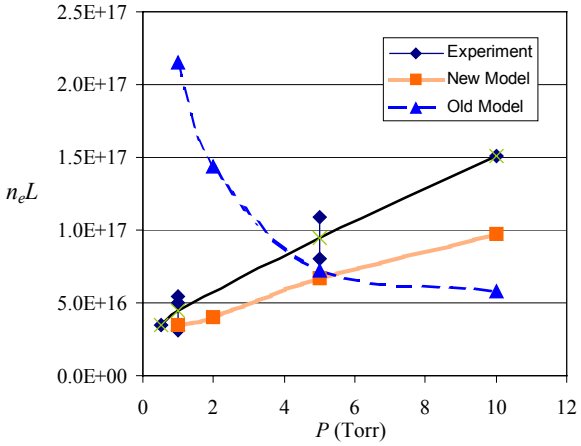

Fig. 3. Final n_e for various background pressures in a ring-diode cell, comparing new and old LSP models with experiment.

current *density*. The experimental ring diode is in fact composed of two thin emitting cathode blades, whereas we have simulated it as a single broad annulus, carrying the same total current but at lower current density. Future simulations will consider this possibility.

The paraxial diode experiment[1] achieves higher current densities, and since this produces electron temperatures on the order of 10 eV and $\langle z \rangle \gg 1$, is a stricter test of the model's severe-perturbation physics. The strong experimental dependence of electron density on beam current density—recall that $P_\Omega \propto j_p^2$—is closely reproduced in the model. Experimentally, it is found that at 1 Torr, reducing the peak current by a factor of two (30 to 15 kA) decrease the line-integrated density from 1.5×10^{17} cm^{-2} to 0.4×10^{17} cm^{-2}. The simulation model, for similar parameters (25 to 15 kA), found a density decrease from 0.9×10^{17} cm^{-2} to 0.3×10^{17} cm^{-2}.

Experimentally, some paraxial electron density histories show a "knee": after increasing slowly at first, the line-integrated density begins to increase rapidly. Figure 4 shows experimental and simulated interferometric densities for 5 Torr air with similar parameters. The knee is reproduced both in temporal location and magnitude.

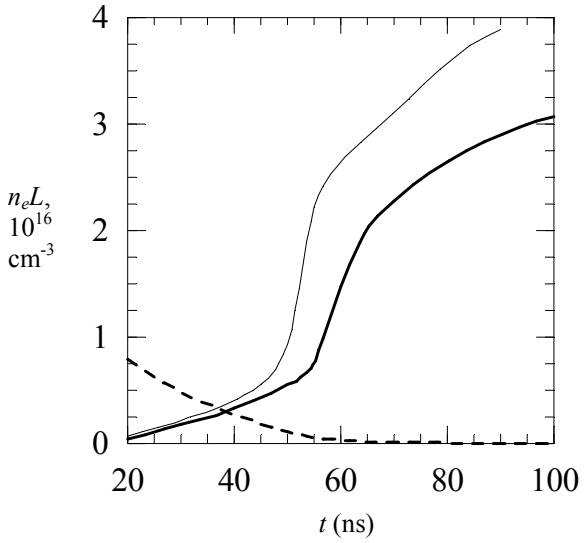

Fig. 4. Experimental and simulated n_eL showing "knee" in time history coinciding with gas dissociation.

Superimposed is the molecular fraction, $1–f_d$, indicative of the power being lost to molecular degrees of freedom, showing that the initial slow-growth phase is likely caused by the diversion of power into vibrational modes, which ceases when the gas is fully dissociated.

The multichord interferometer, which spatially resolves the transport cell, indicates that the electron channel is broad and flat, having a diameter of 1.3 cm, but widening at late times. Initial simulations show a more complicated picture: at early times the electron density is sharply peaked at the beam axis, but as the high ionization potential energy limits further local escalation in $\langle z \rangle$ near the center, regions away from the axis catch up in electron density. Eventually, after the beam current peak, a broad channel of width 0.7 cm is formed.

Simulation and experiment agree on the general dependence of line-integrated electron density on background pressure, as well. At 1 Torr, experimental results indicate a value of 1.5×10^{17} cm^{-2}, while simulations show 0.9×10^{17} cm^{-2}. At 5 Torr, the experimental and simulated values are 3.2×10^{17} cm^{-2} and 2.7×10^{17} cm^{-2}, respectively.

V. SUMMARY

Details of a strongly-perturbed beam-plasma model have been presented, as well as results of initial simulations and comparisons with experiment. In addition to following many neutral, charged, molecular and atomic species, energy equations with ohmic heating, interspecies equilibration, radiation, molecular excitation, and ionization energy sinks have been used to determine the temperature evolution in a manner more relevant to strongly-disturbed gases than the local-field approximation.

A simulation code with beam physics and plasma chemistry allows the modeling of intense charged-particle beam transport environments such as the paraxial diode gas cell. Simulations agree with interferometric measurments in the magnitude of n_eL and in some details of its time history. The dependence of electron density on pressure compares well with experiment.

Future work will expand on these results, considering more experimental data such as net current measurements, and examining the possibility of alternate geometries and pre-ionization of the transport channel.

VI. REFERENCES

[1] D. D. Hinshelwood, *et al.*, "Electron-beam transport studies for radiographic applications," these proceedings.

[2] T. J. Goldsack *et al.*, "Multimegavolt Multiaxis High-Resolution Flash X-Ray Source Development," IEEE Trans. Plasma Sci. **30**, 239 (2002).

[3] T. P. Hughes, R. E. Clark, and S. S. Yu, Phys. Rev. ST Accel. Beams **2**, 110401 (1999).

[4] S. Strasburg, "Intense electron-beam ionization physics in air," Phys. Plasmas, to be published (2003).

[5] R. D. Taylor and A. W. Ali, "Collisional-radiative ionization and recombination model," J. Appl. Phys. **65**, 89 (1988).

[6] D. Mosher, "Coronal equilibrium model for high-z materials," Phys. Rev. A **10**, 2330 (1974).